Desalination and Water Treatment
www.deswater.com

doi:10.5004/dwt.2019.24333

160 (2019) 316–324
August

Comparison for adsorption of tetracycline and cefradine using biochar derived from seaweed *Sargassum* sp.

Gangfu Song[a,b], Yujie Guo[a,b], Guoting Li[a,b,*], Weigao Zhao[c], Yang Yu[d,*]

[a]*Department of Environmental and Municipal Engineering, North China University of Water Resources and Electric Power, Zhengzhou 450011, China, email: sgf@ncwu.edu.cn (G. Song), guoyujie@ncwu.edu.cn (Y. Guo), Tel. +86-371-69127436, Fax +86-371-65790239, email: lipsonny@163.com (G. Li)*
[b]*Henan Key Laboratory of Water Environment Simulation and Treatment, North China University of Water Resources and Electric Power, Zhengzhou 450011, China*
[c]*School of Environmental Science and Engineering, Tianjin University, Tianjin 300072, China, email: zhaoweigao@tju.edu.cn (W. Zhao)*
[d]*Guangdong Key Laboratory of Environmental Pollution and Health, and School of Environment, Jinan University, Guangzhou 510632, China, Tel. +86-371-69127436, Fax +86-371-65790239, email: yuyang@jnu.edu.cn (Y. Yu)*

Received 27 September 2018; Accepted 27 April 2019

ABSTRACT

Surface properties of biochars derived from seaweed *Sargassum* sp. were observed as obvious difference to those from agricultural wastes. In this study, the adsorptive removal of two types of antibiotics, tetracycline (TC) and cefradine (CF), on the biochar were compared and discussed herein. The rod-like tissues of the raw seaweed swelled to be spindle-like at pyrolytic temperature above 400°C. The carbon content was increased from 22.9% of the raw seaweed to 37.2% of the biocharpyrolyzed at 600°C (BC600), while the oxygen content was just increased slightly from 24.7% to 27.8%. The uptake of both TC and CF on the biochar was found to be pH-dependent. The maximum adsorption capacities of TC and CF calculated from the Langmuir model were 128.1 and 61.7 mg/g, respectively, while more CF molecules were adsorbed on biochar at a low adsorbate concentration. Both the Coulombic interaction and π–π electron-donor-acceptor interaction between seaweed biochar and CF/TC molecules played the predominant roles during the adsorption process. The experimental data was well fitted by the pseudo-second-order kinetics model, indicating a possible chemisorption process to some extent. Isotherm result implied that both surface adsorption and partitioning contributed to the uptake of TC and CF onto BC600.

Keywords: Adsorption; Seaweed biochar; Tetracycline; Cefradine; Mechanism

1. Introduction

As one of the most attractive water treatment technologies, adsorption process has been studied and applied for practical treatment. During the adsorption process, pollutants could be concentrated and adsorbed on the adsorptive materials without generation of any toxic intermediates, and further separated from treated water via filtration or centrifugation [1,2]. As such, numerous adsorbents have been developed for removing inorganic contaminants (e.g., heavy metals, arsenic and fluoride) and organic contaminants (e.g., dyes) from water. On the other hand, to evaluate the removal efficiency of contaminant degradation from aqueous medium, electrochemical sensors as a new approach developed which is relatively cheaper compared to the other common analytical methods such as atomic absorption spectroscopy (AAS), inductively coupled plasma optical emission and mass spectroscopy (ICP-OES and ICP-MS) and ion chromatography (IC) and applied widely as sensitive diagnostic tools recently [3–10].

Carbon-based adsorbents are generally advantageous for removing organic pollutants due to their large surface area, high affinity towards organic matters and ease of regeneration. Among them, low-cost biochars derived from

*Corresponding author.

natural biomasses or agricultural wastes have attracted increasing attention on their performance of water treatment. The preparation of biochar offers the chance to turn bioenergy into a carbon-negative industry, with carbon sequestration and gas capture, which are expected to be a carbon-neutral energy source [11,12]. On the other hand, biochar has shown promising application potential in environmental management, including soil improvement, waste management, climate change mitigation, and energy production [13–15]. In particular, biochar is also considered as an environmentally friendly adsorbent for adsorptive removal of organic/inorganic contaminants from soil and water [16–18]. Various biomasses such as agricultural wastes have been reportedly utilized to prepare biochar with a great adsorption capability of organic pollutants. Even though, the raw biochar has limited ability to adsorb contaminants from aqueous solution while the adsorption capability for various contaminants depends on its physical and chemical properties affected by feed stocks, pyrolysis technologies and pyrolysis conditions [19].

Further, the study on the adsorptive performance of biochar derived from marine biomasses, e.g., seaweed, has not yet been fully reported. Abundant marine biomasses are expected to be utilized as low-cost adsorbent for the management of various environmental contaminants. Seaweed *Sargassum* sp., as an ideal biosorbent that has a fiber-like structure and an amorphous embedding matrix of various polysaccharides as well as some highly complex organic compounds both within the cell wall and in the intercellular substance, can effectively remove heavy metal ions with concentrations ranging from few ppm to several hundreds ppm [20–23]. Since the possible organic leaching from *Sargassum* sp. and the resulting secondary pollution problem, direct application of raw seaweeds for the adsorptive removal of organic contaminants is lack of practical application potential. In view of the unique characteristics of *Sargassum* sp., the biochar derived from *Sargassum* sp.is expected to have a novel porous micro-structure and large surface area, which could help enhance the adsorptive removal of contaminants accordingly. Therefore, the modification or conversion of *Sargassum* sp. prior to application is a better choice to develop more stable and efficient adsorbents for removing organic contaminants.

In our previous study, layered carbon particles synthesized by using concentrated acid to carbonize seaweed *Sargassum* sp. have shown excellent adsorptive capability despite of the high cost for the carbon particle preparation [24,25]. Meanwhile, pharmaceutical and personal care products (PPCPs) have attracted wide attention in recent studies [26–31]. As antibiotics are not easily biodegradable and can cause numerous ecological impacts, residual antibiotics are capable of increasing the antibiotic resistance of bacteria in marine ecosystems, while bioaccumulation and biomagnification in aquatic organisms are another major ecological impact of residue antibiotics [32–34]. Antibiotics, tetracycline and cefradine have similar molecular weight while their functional groups are largely different. It might be interesting to compare their adsorption performance and explore some significant results. In this study, seaweed biochar was developed via a simple and cost-effective pyrolysis method, and innovatively applied for adsorptive removal of two typical emerging PPCPs, tetracycline and cefradine. A series of batch experiments were conducted to evaluate and compare the adsorption performance of tetracycline and cefradine on seaweed biochar in this paper, and the adsorption mechanism was discussed as well.

2. Materials and methods

2.1. Materials and apparatus

Tetracycline hydrochloride (TC, molecular weight 444) was purchased from Solar biolife sciences company (Beijing, China). Cefradine (CF, molecular weight 349) was from Tianjin Fengfan chemical reagent company (Tianjin, China). Both TC and CF were used without further purification. Other chemicals used were of analytical grade. Deionized (DI) water was used to prepare all solutions.

2.2. Preparation of seaweed biochar

Seaweed *Sargassum* sp. was collected from the west coast of Singapore. The seaweed biomass was washed, dried, crushed and sieved using a 40 mesh sieve. The pretreated biomass was put into a ceramic pot with pressed state and covered with a fitting lid. Under an oxygen-limited condition, the biomass was pyrolyzed at different temperatures for 3 h. The resultant biochar was placed in a 4 mol/L HCl solution for 12 h and separated by filtration. Then, the biochar residues were rinsed with DI water until a neutral solution pH was achieved. The product was subsequently oven-dried overnight at 80°C. The treated biochar was finally preserved in a desiccator for further use. The seaweed biochars pyrolyzed at 400°C and 600°C were designated as BC400 and BC600, respectively.

2.3. Batch adsorption experiment

The stock solutions of TC and CF (500 mg/L) were freshly prepared by respectively dissolving a certain amount of TC and CF in DI water and then stored in a refrigerator at 277 K. The working solutions with desired concentrations of TC and CF were prepared by diluting stock solutions with DI.

In the experiments of pH effect and adsorption isotherm, the concentration of TC or CF was 20 mg/L, and the dose of seaweed biochar was 0.4 g/L. After shaking at 145 rpm for 24 h, samples were collected and filtered through a 0.45 μm syringe membrane filter before concentration measurement. The reaction temperature was kept constant at 298 K. Solution pH adjustment was effected by the addition of a diluted HNO_3 or NaOH at neutral pH except during the pH effect study itself. For the kinetics study, 400 mg of seaweed biochar was added into 1000 mL of 20 mg/L TC or CF solution.

2.4. Regeneration and reuse of biochar

The exhausted seaweed biochar BC600 was separated from the previous experiments, washed by DI water and dried at room temperature. Then, 100 mg of the exhausted biochar BC600 was added into 300-mL conical flask containing 150-mL solution with different concentrations of NaOH or HCl (0.01 and 0.1 M). The mixtures were agitated at 120

rpm for 6 h at room temperature. After that, the biochar was collected, washed by DI water to neutral pH conditions and dried at 353 K for next cycle of adsorption experiment.

2.5. Characterization of biochar

The surface morphologies of the raw seaweed and seaweed biochars pyrolyzed at different temperatures were observed by a scanning electron microscope (SEM) coupled with an energy dispersive X-ray (EDX) spectrometer (Philips Quanta 2000, Netherlands). The specific surface areas of biochars were measured by the Brunauer, Emmett and Teller (BET) method via a surface area and pore-size analyzer (NOVA 2200 e, USA). Fourier transform infrared spectroscopy (FTIR) spectra were recorded on a Nicolet NEXUS 470 FTIR spectrophotometer. The samples were prepared in the form of KBr pellets and scanned in a range of 400 to 4000 cm^{-1}. The zeta potential of biochar pyrolyzed at 600°C was determined by using a zeta potential analyzer (Zetasizer 2000, Malvern Co., UK). The particle concentration of the biochar in the testing solution was 200 mg/L. $NaNO_3$ was used as a background electrolyte to maintain an appropriately constant ionic strength of 0.01 M. After being mixed for 48 h, 20 mL of suspension was transferred to a sample tube. The zeta potential was then measured by electrophoresis analysis.

2.6. Concentration analysis

The concentrations of TC and CF were analyzed using an UVmini-1240 spectrophotometer (Shimadzu, Japan) by monitoring emissions at the wavelength of maximum absorption at 360 and 264 nm, respectively [35,36].

The adsorption capacities were calculated as following:

$$q_e = (C_0 - C_e)V/W \quad (1)$$

$$q_t = (C_0 - C_t)V/W \quad (2)$$

where q_e and q_t (mg/g) are the adsorption capacities at equilibrium and time t (min); C_0 (mg/L) is the initial concentration of TC or CF in solution, while C_e and C_t (mg/L) are the concentrations of TC or CF at equilibrium and t (min), respectively; V (L) is the volume of solution, and W (g) is the mass of the seaweed biochar used.

3. Results and discussion

3.1. Characterization of the seaweed biochar

3.1.1. SEM and EDX

The SEM images of the raw seaweed *Sargassum* sp., and the seaweed biochars pyrolyzed at 400°C (BC400) and 600°C (BC600) are presented in Fig. 1. From Fig. 1a and 1b, it can be found that the compact raw seaweed was composed of rod-like and granular tissues. The length of rods was within 20 μm while the size of particles was below 2 μm. After pyrolysis at 400°C, the rod-like tissues seemed to become spindle-like particles with more well-defined structure and no granular particles fully is shown in Fig. 1c. As shown in Fig. 1d, the spindle-like particles was further carbonized and destroyed at pyrolysis temperature of 600°C, resulting in a more compacted structure of seaweed biochar.

As presented in Fig. 2, the element contents of C, N and O, and the molar ratios of O/C and (O + N)/C in the raw seaweed, BC400 and BC600 were roughly determined by EDX. It is worth to note that the carbon contents of raw seaweed, BC400 and BC600 were not as high as expected, with carbon contents increasing from 22.9% of the raw seaweed to 37.2% of BC600, which were only about half of those from the raw bagasse and the related biochars reported in our previous study [37]. The low carbon contents in raw seaweed and BC600 might be due to the presence of plentiful polysaccharide and protein within the raw seaweed. The adsorption performance of the seaweed and the related biochars might be therefore of obvious difference with the agricultural waste and related biochars. Similarly, the N and O contents increased from 2.9% and 24.7% of the raw seaweed to 4.1% and 27.8% of the seaweed biochar BC600, respectively. The relative molar ratios of O/C and (O+N)/C before and after pyrolysis treatment could reflect the change of surface hydrophilicity and functional groups of the seaweed and biochars to some extent. After the pyrolysis at 600°C, the molar ratios of O/C and (O+N)/C decreased from 81.2% to 56.2% and from 92.2% to 65.7%, respectively. The reduction of O/C molar ratio indicated that the biochar surface became less hydrophilic, while the decrease of (O+N)/C molar ratio, a polarity index implied the loss of the surface polar functional groups [38–40]. Compared to the bagasse and the related biochars, seaweed and BC600 had higher molar ratios of O/C and (O+N)/C, suggesting that biochar derived from seaweed could retain more polar functional groups on the surface and facilitate the diffusion and adsorption of polar organic pollutants on the biochar surface.

3.1.2. BET surface area

BET surface areas and average pore sizes of the raw seaweed, and seaweed biochar BC400 and BC600 were measured and are presented in Fig. 3. Generally, the surface area of biomass could significantly increase after pyrolysis treatment at high temperatures. As illustrated in Fig. 3, the BET surface areas of BC400 and BC600 respectively reached 10.58 and 10.68 m^2/g, nearly 15 times higher than that of raw seaweed (0.68 m^2/g), although these values were not so high as those of other biochars previously reported. Different from the surface areas, the average pore size of seaweed biomass increased from 6.58 nm to 7.41 nm after pyrolysis treatment at 400°C, and further increased to 7.95 nm for BC600. Thus, the pyrolysis temperature raised from 400°C to 600°C seemed to have a neglectable effect on the enhancement of special surface area of biochar but could further increase the average pore size.

3.1.3. FTIR

The FTIR spectra of the raw seaweed and seaweed biochar samples prepared at different pyrolytic temperatures are shown in Fig. 4. The strong band at 3417 cm^{-1} was assigned to the stretching vibration of hydroxyl groups. The band strength gradually reduced with increasing

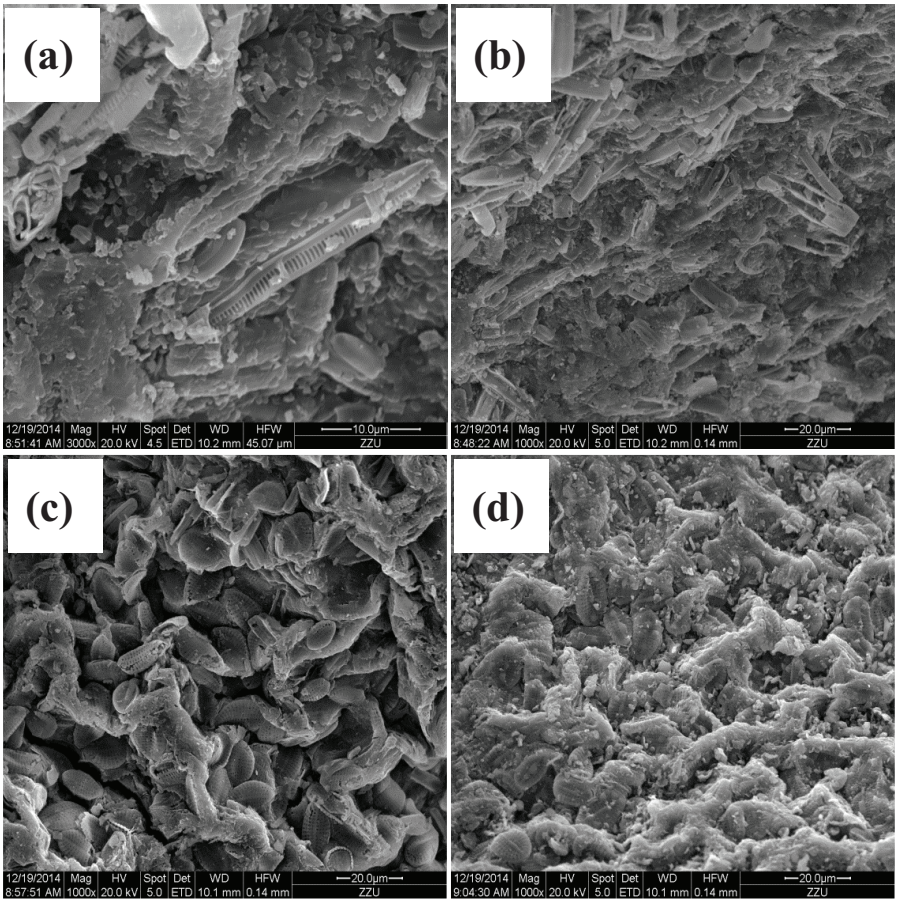

Fig. 1. Scanning electron microscopy images of the raw seaweed (a,b) and seaweed biochar BC400 (c) and BC600 (d).

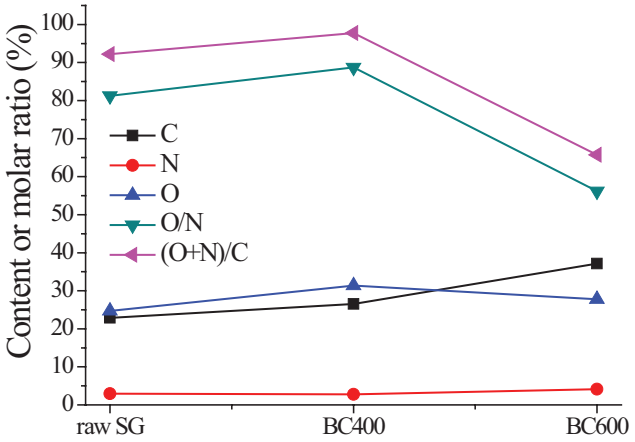

Fig. 2. Changes in element contents (wt%) of C, N, O and the molar ratios (%) of O/C and (O+N)/C in the raw seaweed, and seaweed biochar BC400 and BC600.

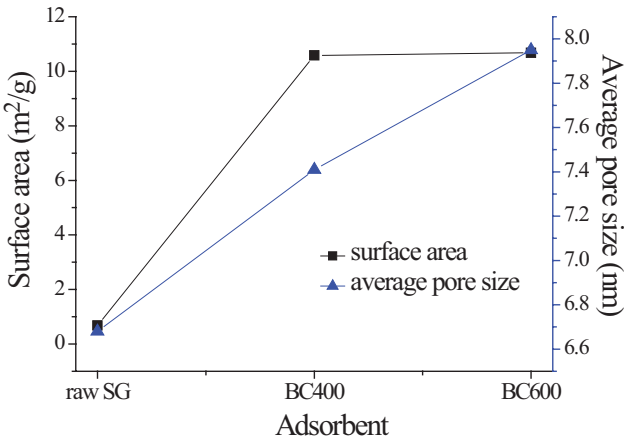

Fig. 3. BET surface areas and average pore sizes of the raw seaweed, seaweed biochar BC400 and BC600.

pyrolytic temperature, indicating the significant loss of moisture and water of hydration due to pyrolysis process. The bands at 2920 cm^{-1} (aliphatic C-H stretching), 1640 cm^{-1} and 1418 cm^{-1} (-COOH stretching) nearly disappeared when pyrolysis temperature were higher than 400°C [20]. A new band at 1723 cm^{-1} assigned to C=O group appeared at 200 and 300°C but diminished and disappeared at 500°C and 600°C, which was also observed by other researchers [41,42]. This implied that the maximum content of C=O functional groups on the biochar surface could be achieved during the pyrolysis process at around 300°C, which might be responsible for the change of oxygen content on the biochars.

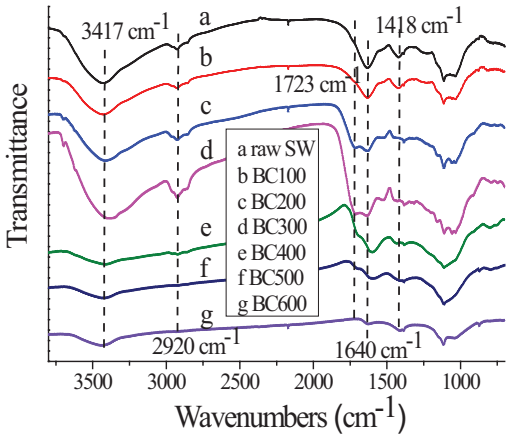

Fig. 4. FTIR spectra of the raw seaweed (SW), and seaweed biochar samples prepared under pyrolysis temperatures from 100°C to 600°C.

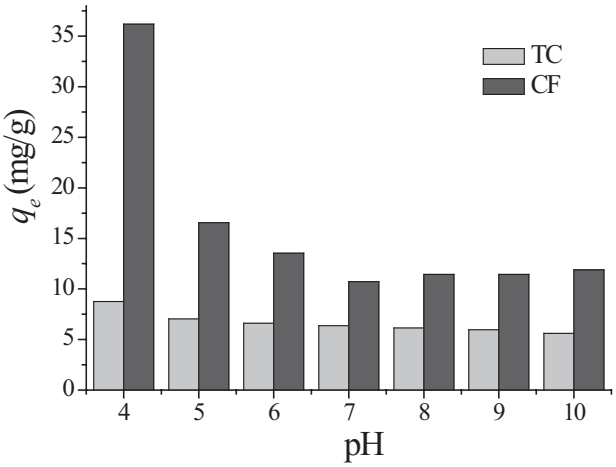

Fig. 5. Effect of solution pH on the adsorption of TC and CF by using BC600.

3.2. Effect of solution pH on the adsorption of TC and CF

On the basis of the stability and surface properties of seaweed biochars, BC600 was selected to evaluate the adsorption performance of TC and CF. The effect of solution pH was conducted in the pH range of 4.0 to 10.0 and results were shown in Fig. 5. The adsorption of TC and CF was found to be highly pH-dependent and the acidic condition was favorable for the contaminants uptake. The variation of uptake at different pH indicated that H-bond was formed during adsorption. The optimal adsorption was achieved at pH 4.0 for both TC and CF with the adsorption capacities of 8.8 and 36.2 mg/g, respectively, and gradually decreased with the increase in solution pH. The uptake of CF was higher than that of TC in the testing pH range.

Generally, the surface charge of the biochar should be greatly affected by solution pH and a more negatively-charged biochar surface is theoretically favorable for the adsorption of positively charged pollutants due to Coulombic attraction [5]. Zeta potential of the biochar BC600 as s function of solution pH is presented in Fig. 6. The surface charge in the pH range of 3.0~10.0 turned to be more negative with the increasing solution pH. Compared to bagasse biochar pyrolyzed at 600°C reported in our previous study, biochar derived from seaweed at the same pyrolysis temperature (BC600) seemed to have a relatively lower surface charge, indicating the surface properties of biochar could be determined by their biomass precursor.

Although TC and CF have similar molecular weight, they would exist in different ionic forms in water due to protonation or deprotonation of their different functional groups at different pHs. Amphoteric TC molecules may mainly exist in a cationic form at pH < 3.3, resulting from the protonation of dimethylammonium group. At the pH ranging from 3.3 to 7.68, it would present as a zwitter ion due to the loss of proton from the phenolic diketone moiety. At pH > 7.68, it mainly exists as an anion when the tricarbonyl system and phenolic diketone moiety deprotonated [43,44]. In contrast, the CF molecules containing typical functional groups,including aminogroup and carboxyl group, have pK_a values of 7.3 and 2.5. It was therefore

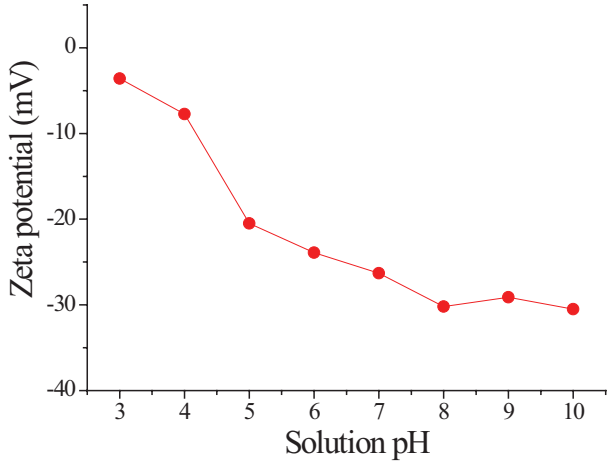

Fig. 6. Zeta potentials of seaweed biochar BC600. Biochar dose = 200 mg/L, ionic strength 0.01 M $NaNO_3$, equilibrium time 48 h.

deduced that CF molecules could become more negatively charged at lower solution pH than TC. Compared to TC, a lower uptake of CF was expected as a consequence of a higher Coulombic repulsion force between CF and BC600. However, the uptake of CF was higher than that of TC within the whole pH range examined. Additionally, there was similar difference on the adsorption performance of BC 600 for both CF and TC at pH > 7 in which the Coulombic repulsion between BC600 and CF/TC molecules should be enhanced with the increasing pH. So it could be concluded that the Coulombic interaction between seaweed biochar and CF/TC molecules would slightly affect the adsorption process.

Since the seaweed biochar BC600 had a highly graphitized surface with relatively high π-electron density, it could work as π-electron donors. TheTC and CF molecules were generally regarded as π-electron acceptors, leading to a mechanism of π–π electron-donor-acceptor (EDA) interaction involved in the enhancement of adsorption onto BC600

[45–47]. As the protonated and neutral species of TC and CF were more effective π-electron acceptors, a slight reduction in TC and CF uptake was expected under alkaline conditions. This was consistent with results from the pH effect study. Thereby, it was deduced that the EDA interaction between BC600 and CF is stronger than that between BC600 and TC, yielding a comparatively higher uptake of CF on BC600.

3.3. Adsorption kinetics

Adsorption kinetics of TC and CF onto the seaweed biochar BC600 was investigated at pH 5.0, 7.0 and 9.0, respectively. Similar adsorption kinetics performances were observed for both antibiotics. For simplicity, only the adsorption kinetics of TC is presented in Fig. 7. Two kinetics models including pseudo-first-order and pseudo-second-order models were used to fit the kinetics data. The mathematical equations of the linear and non-linear models of the pseudo-first-order and the pseudo-second-order kinetics are those available in the literature [48,49]:

$$q_t = q_e(1 - e^{-k_1 t}) \tag{3}$$

$$\ln(q_e - q_t) = \ln q_e - k_1 t \tag{4}$$

$$q_t = \frac{k_2 q_e^2 t}{(1 + k_2 q_e t)} \tag{5}$$

$$\frac{t}{q_t} = \frac{1}{k_2 q_e^2} + \frac{t}{q_e} \tag{6}$$

where q_e and q_t are the adsorption capacities (mg/g) at equilibrium and at time t (minutes), respectively; and k_1 (min^{-1}) and k_2 (g/mg·min) are the related adsorption rate constants for the pseudo-first-order and the pseudo-second-order model, respectively.

The linear and non-linear kinetic parameters for the adsorption of TC are presented in Table 1. Based on the correlation coefficients (R^2), the experimental data can be better fitted by the pseudo-second-order kinetics model in both linear and nonlinear forms, indicating that the uptake of TC onto the seaweed biochar might be a chemisorption process to some extent. According to the values of k_2, the adsorption of TC on seaweed biochar BC600 at pH 7.0 was relatively faster than that at pH 5 and 9. This was beneficial for its practical application on the treatment of contaminated natural water (pH at around 6.8).

3.4. Adsorption isotherms

Adsorption isotherm study can provide key information for the surface properties and the adsorption behaviour of an adsorbent. The isotherm data was simulated by both the Langmuir and the Freundlich isotherm models. The saturated monolayer Langmuir isotherm can be represented as [50]:

$$q_e = \frac{q_m k_L C_e}{1 + k_L C_e} \tag{7}$$

where q_e is the amount of antibiotics adsorbed onto BC600 (mg/g), C_e is the equilibrium concentration (mg/L), q_m is the maximal adsorption capacity of BC600 (mg/g) and k_L is the equilibrium adsorption constant related to the affinity of binding sites (L/mg).

The Freundlich isotherm is an empirical equation most-widely used in describing adsorption on a heterogeneous surface. It is commonly described as [51]:

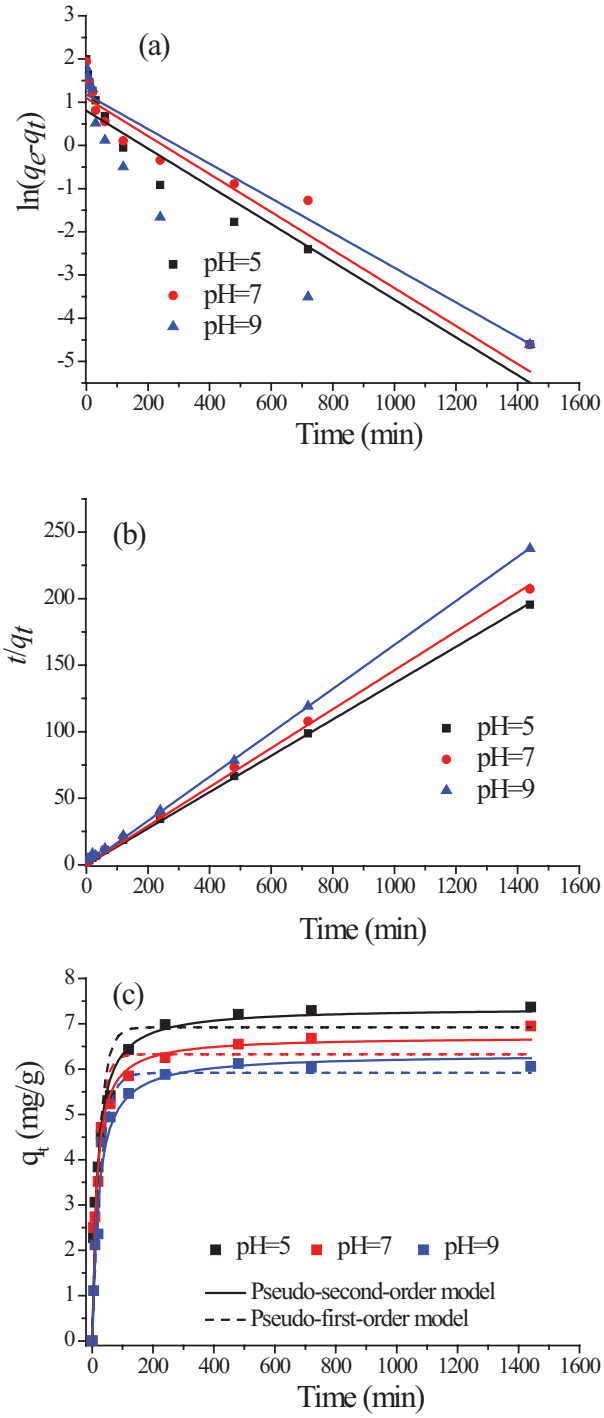

Fig. 7. Linear (a, b) and nonlinear (c) adsorption kinetics for the pseudo-first-order and the pseudo-second-order simulations of TC onto the seaweed biochar BC600.

Table 1
Linear and non-linear kinetics parameters for the adsorption of TC onto the seaweed biochar BC600

Model	pH = 5	pH = 7	pH = 9
Linear pseudo-first-order model			
k_1 (min^{-1})	0.0044	0.00401	0.00437
q_e (mg/g)	2.99	3.36	2.23
R^2	0.902	0.939	0.816
Linear pseudo-second-order model			
k_2 (g/mg·min)	0.0163	0.0229	0.0144
q_e (mg/g)	5.73	6.01	6.06
R^2	0.999	0.999	0.999
Nonlinear pseudo-first-order model			
k_1 (min^{-1})	0.0413	0.0481	0.0351
q_e (mg/g)	6.92	6.33	5.92
R^2	0.942	0.933	0.975
Nonlinear pseudo-second-order model			
k_2 (g/mg·min)	0.00837	0.0107	0.00769
q_e (mg/g)	7.35	6.71	6.33
R^2	0.988	0.979	0.976

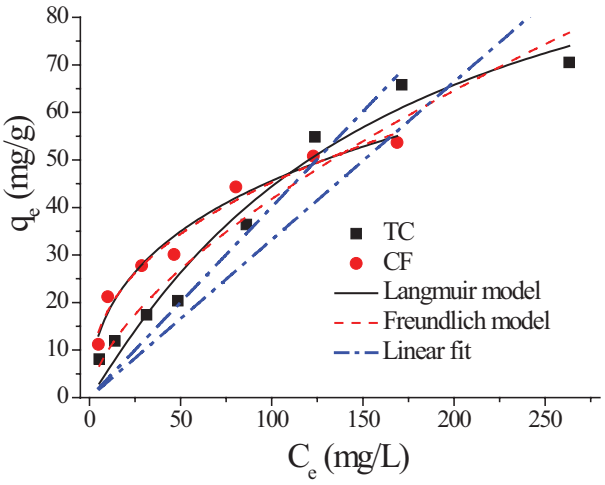

Fig. 8. Adsorption isotherms for TC and CF at 298 K and simulated curves by Langmuir, Freundlich model and linear fit.

$$q_e = k_F C_e^{\frac{1}{n}} \quad (8)$$

where k_F(mg$^{(1-1/n)}$L$^{1/n}$/g) and n are the Freundlich constants related to the adsorption capacity and adsorption intensity of the adsorbent, respectively.

The adsorption isotherms for TC and CF onto the seaweed biochar BC600 at 298 K and the fitting lines from both the Langmuir and the Freundlich models are shown in Fig. 8. According to the parameters listed in Table 2, both the Langmuir and the Freundlich models seemed to work well for fitting the experimental data as the experimental points were quite close to the simulated curves and R^2 values with both models were acceptable (higher than 0.92).The maximum adsorption capacities calculated from the Langmuir model for TC and CF were 128.1 and 61.7 mg/g, respectively. Note that a higher adsorption capacity of CF could be obtained at low equilibrium concentration than that of TC.

Since the relative contribution of adsorption could be increased with increasing pyrolytic temperature, the contribution from the adsorption was shown to be higher than that of partitioning to total sorption for the biochars of orange peel treated under comparatively higher temperatures (>500°C) [38]. As presented in Fig. 8, linear simulation of the adsorption isotherm data for the two antibiotics were also conducted. The R^2 values for the uptake of TC and CF were 0.939 and 0.865, respectively, indicating that the adsorption curves for both antibiotics were quasi-linear and partition mechanism plays a certain role in the adsorption process as well.

3.5. Regeneration and reuse

The seaweed biochar of BC600 after the adsorption was collected, washed and added into different regenerating solutions, e.g., NaOH or HCl (0.01 and 0.1 M), to evaluate its regeneration and reusability. After regenerating for 6 h, the biochar was used for next cycle of adsorption experiment. As shown in Fig. 9, the removal efficiency of regenerated biochars by using 0.1 M HCl, 1 M HCl, 0.1 M NaOH and 1 M NaOH as regenerating solutions could achieve 89.2%, 90.0%, 91.2% and 90.3%, respectively. The solution of 0.1 M NaOH had a slightly better performance to regenerate the seaweed biochar and it was recommended to regenerate the spent biochar Accordingly, the removal efficiency of biochars regenerated in three cycles could reach 91.2%, 88.9% and 84.7%, respectively.

4. Conclusion

Seaweed biochar prepared through a simple pyrolysis process was applied for comparative adsorption removal of antibiotics tetracycline (TC) and cefradine (CF). The spindle-like morphology of prepared biochar pyrolyzed at 600°C (BC600) had a more compacted structure. The biochar became more hydrophobic and carbon-rich with increasing pyrolytic temperature. The uptake of both TC and CF decreased gradually with increasing solution pH while the uptake of CF was evidently higher than that of TC at a low

Table 2
Langmuir and Freundlich isotherm parameters for the adsorption of TC and CF on BC600 at 298 K

	Langmuir isotherm			Freundlich isotherm		
	q_m (mg/g)	k_L (L/mg)	R^2	k_F (mg$^{(1-1/n)}$L$^{1/n}$/g)	n	R^2
TC	128.1	0.00524	0.964	2.31	0.629	0.949
CF	61.7	0.0316	0.920	7.34	0.395	0.967

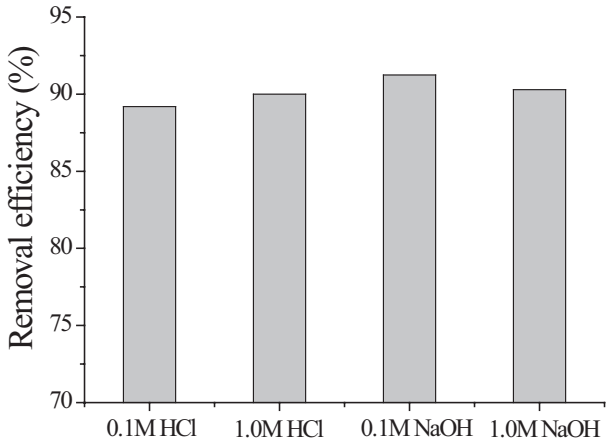

Fig. 9. Removal efficiency using seaweed biochar BC600 regenerated in different solutions.

adsorbate concentration. Based on the results of pH effect, zeta potential of biochar and species distribution of TC/CF under different solution pH, effect of Coulombic force between biochar and TC/CF on the adsorption should be neglectable. The π–π electron-donor-acceptor (EDA) interaction between BC600 and CF was stronger than TC, yielding a comparatively higher adsorption capacity of CF on BC600. Kinetics data can be fitted better by the pseudo-second-order kinetic model, indicating a possible chemisorptions process to some extent. Isotherm study suggested that both surface adsorption and partitioning contributed to the uptake of TC and CF onto BC600.

Acknowledgment

The Authors are grateful for financial support from the National Natural Science Foundation of China (Grant no. 51378205).

References

[1] I. Ali, M. Asim, T.A. Khan, Low cost adsorbents for the removal of organic pollutants from wastewater, J. Environ. Manage., 113 (2012) 170–183.
[2] J.H. Qu, Research progress of novel adsorption processes in water purification, J. Environ. Sci., 20 (2008) 1–13.
[3] S. Ahmadzadeh, M. Rezayi, E. Faghih-Mirzaei, M. Yoosefian, A. Kassim, Highly selective detection of titanium (III) in industrial wastewater samples using meso-octamethylcalix[4] pyrrole-doped PVC membrane ion-selective electrode, Electrochim. Acta, 178 (2015) 580–589.
[4] S. Ahmadzadeh, M. Rezayi, A. Kassim, M. Aghasi, Cesium selective polymeric membrane sensor based on p-isopropylcalix [6] arene and its application in environmental samples, RSC Adv., 5 (2015) 39209–39217.
[5] S. Ahmadzadeh, M. Rezayi, H. Karimi-Maleh, Y. Alias, Conductometric measurements of complexation study between 4-isopropylcalix [4]arene and Cr^{3+} cation in THF–DMSO binary solvents, Measurement, 70 (2015) 214–224.
[6] S. Ahmadzadeh, A. Kassim, M. Rezayi, A conductometric study of complexation reaction between meso-octamethylcalix[4]pyrrole with titanium cation in acetonitrile-ethanol binary mixtures, Int. J. Electrochem. Sci., 6 (2011) 4749–4759.
[7] A. Kassim, M. Rezayi, S. Ahmadzadeh, G. Rounaghi, M. Mohajeri, N.A. Yusof, T.W. Tee, L.Y. Heng, Abd.H. Abdullah, A Novel ion-selective polymeric membrane sensor for determining thallium (I) with high selectivity, IOP Conference Series: Mater. Sci. Eng., IOP Publishing, 17 (2011) 012010.
[8] S. Ahmadzadeh, F. Karimi, N. Atar, E.R. Sartori, E. Faghih-Mirzaei, E. Afsharmanesh, Synthesis of CdO nanoparticles using direct chemical precipitation method: Fabrication of novel voltammetric sensor for square wave voltammetry determination of chlorpromazine in pharmaceutical samples, Inorga. Nano-Met. Chem., 47(3) (2017) 347–353.
[9] J.P. Unyimadu, O. Osibanjo, J.O. Babayemi, Selected persistent organic pollutants (POPs) in water of River Niger: occurrence and distribution, Environ. Monit. Assess., 190 (2018) 340(6).
[10] Y. Abdollahi, A.H. Abdullah, U.I. Gaya, S. Ahmadzadeh, A. Zakaria, K. Shameli, Z. Zaina, H. Jahangirian, N.A. Yusof, Photocatalytic degradation of 1,4-benzoquinone in aqueous ZnO dispersions, J. Brazil. Chem. Soc., 23(2) (2012) 236–240.
[11] J. Lehmann, A handful of carbon, Nature, 447 (2007) 143–144.
[12] J.W. Lee, B. Hawkins, D.M. Day, D.C. Reicosky, Sustainability: the capacity of smokeless biomass pyrolysis for energy production, global carbon capture and sequestration, Energ. Environ. Sci., 3 (2010) 1695–1705.
[13] M. Ahmad, A.U. Rajapaksha, J.E. Lim, M. Zhang, N. Bolan, D. Mohan, M. Vithanage, S.S. Lee, Y.S. Ok, Biochar as a sorbent for contaminant management in soil and water: A review, Chemosphere, 99 (2014) 19–33.
[14] Y. Zhou, L. Zhang, Z.J. Cheng, Removal of organic pollutants from aqueous solution using agricultural wastes: A review, J. Mol. Liq., 212 (2015) 739–762.
[15] A.U. Rajapaksha, S.S. Chen, D.C.W. Tsang, M. Zhang, M. Vithanage, S. Mandal, B. Gao, N.S. Bolan, Y.S. Ok, Engineered/designer biochar for contaminant removal/immobilization from soil and water: Potential and implication of biochar modification, Chemosphere, 148 (2016) 276–291.
[16] F. Sadegh-Zadeh, A.W. Samsuri, B.J. Seh-Bardan, M. Emadi, The effects of acidic functional groups and particle size of biochar on Cd adsorption from aqueous solutions, Desal. Water Treat., 66 (2017) 309–319.
[17] P. Peng, Y.H. Lang, X.M. Wang, Adsorption behavior and mechanism of pentachlorophenol on reed biochars: pH effect, pyrolysis temperature, hydrochloric acid treatment and isotherms, Ecol. Eng., 90 (2016) 225–233.
[18] Q.M. Cheng, Q. Huang, S. Khan, Y.J. Liu, Z.N. Liao, G. Li, Y.S. Ok, Adsorption of Cd by peanut husks and peanut husk biochar from aqueous solutions, Ecol. Eng., 87 (2016) 240–245.
[19] X.F. Tan, Y.G. Liu, Y.L. Gu, Y. Xu, G.M. Zeng, X.J. Hu, S.B. Liu, X. Wang, S.M. Liu, J. Li, Biochar-based nano-composites for the decontamination of wastewater: A review, Bioresour. Technol., 212 (2016) 318–333.
[20] J.P. Chen, L. Yang, Chemical modification of *Sargassum* sp. for prevention of organic leaching and enhancement of uptake during metal biosorption, Ind. Eng. Chem. Res., 44 (2005) 9931–9942.
[21] E. Romera, F. Gonzalez, A. Ballester, M.L. Blazquez, J.A. Munoz, Comparative study of biosorption of heavy metals using different types of algae, Bioresour. Technol., 98 (2007) 3344–3353.
[22] G. Bayramo-lu, M.Y. Arica, Construction a hybrid biosorbent using scenedesmusquadricauda and Ca-alginate for biosorption of Cu(II), Zn(II) and Ni(II): kinetics and equilibrium studies, Bioresour. Technol., 100 (2009) 186–193.
[23] R.C. Oliveira, P. Hammer, E. Guibal, J.M. Taulemesse, O. Garcia, Characterization of metal-biomass interactions in the lanthanum(III) biosorption on Sargassum sp. using SEM/EDX, FTIR, and XPS: Preliminary studies, Chem. Eng. J., 239 (2014) 381–391.
[24] G.T. Li, Y.P. Guo, W.G. Zhao, Efficient adsorption removal of tetracycline by layered carbon particles prepared from seaweed biomass, Environ. Prog. Sustain., 36(1) (2017) 59–65.
[25] Y. Yu, C.H. Wang,X. Guo, J.P. Chen, Modification of carbon derived from *Sargassum* sp. by lanthanum for enhanced adsorption of fluoride, J. Colloid Interf. Sci., 441 (2015) 113–120.
[26] S. Ahmadzadeh, A. Asadipour, M. Pournamdaric, B. Behnam, H.R. Rahimi, M. Dolatabadi, Removal of ciprofloxacin from

hospital wastewater using electrocoagulation technique by aluminum electrode: Optimization and modelling through response surface methodology, Process Saf. Environ., 109 (2017) 538–547.
[27] S. Ahmadzadeh, M. Dolatabadi, Modeling and kinetics study of electrochemical peroxidation process for mineralization of bisphenol A: a new paradigm for groundwater treatment, J. Mol. Liq., 254 (2018) 76–82.
[28] S. Ahmadzadeh, M. Dolatabadi, Removal of acetaminophen-from hospital wastewater using electroFenton process, Environ. Earth Sci., 77 (2018) 53:1–11.
[29] S. Ahmadzadeh, A. Asadipour, M. Yoosefian, M. Dolatabadi, Improved electrocoagulation process using chitosan for efficient removal of cefazolin antibiotic from hospital wastewater through sweep flocculation and adsorption: kinetic and isotherm study, Desal. Water Treat., 92 (2017) 160–171.
[30] S. Ahmadzadeh, M. Dolatabadi, Electrochemical treatment of pharmaceutical wastewater through electrosynthesis of iron hydroxides for practical removal of metronidazole, Chemosphere, 212 (2018) 533–539.
[31] M. Yoosefian, S. Ahmadzadeh, M. Aghasi, M. Dolatabadi, Optimization of electrocoagulation process for efficient removal of ciprofloxacin antibiotic using iron electrode: kinetic and isotherm studies of adsorption, J. Mol. Liq., 225 (2017) 544–553.
[32] Y. Bai, W. Meng, J. Xu, Y. Zhang, C. Guo, Occurrence, distribution and bioaccumulation of antibiotics in the Liao River Basin in China, Env. Sci. Process. Impact, 16 (2014) 586–593.
[33] L. Gao, Y. Shi, W. Li, J. Liu, Y. Cai, Occurrence, distribution and bioaccumulation of antibiotics in the Haihe River in China, J. Environ. Monit., 14 (2012) 1247–1254.
[34] H.Y. Kim, J. Jeon, J. Hollender, S. Yu, S.D. Kim, Aqueous and dietary bioaccumulation of antibiotic tetracycline in D. Magna and its multigenerational transfer, J. Hazard. Mater., 279 (2014) 428–435.
[35] R.A. Figueroa, A. Leonard, A.A. MacKay, Modeling tetracycline antibiotic sorption to clays, Environ. Sci. Technol., 38 (2004) 476–483.
[36] Z.J. Hu, N.X. Wang, J. Tan, J.Q. Chen, W.Y. Zhong, Kinetic and equilibrium of cefradine adsorption onto peanut husk, Desal. Water Treat., 37 (2012) 160–168.
[37] G.T. Li, W.Y. Zhu, L.F. Zhu, X.Q. Chai, Effect of pyrolytic temperature on the adsorptive removal of p-benzoquinone, tetracycline, and polyvinyl alcohol by the biochars from sugarcane bagasse, Korean J. Chem. Eng., 33(7) (2016) 2215–2221.
[38] B.L. Chen, Z.M. Chen, Sorption of naphthalene and 1-naphthol by biochars of orange peels with different pyrolytic temperatures, Chemosphere, 76 (2009) 127–133.
[39] Y. Chun, G.Y. Sheng, C.T. Chiou, B.S. Xing, Compositions and sorptive properties of crop residue-derived chars, Environ. Sci. Technol., 38 (2004) 4649–4655.
[40] G. Cornelissen, O. Gustafsson, Importance of unburned coal carbon, black carbon, and amorphous organic carbon to phenanthrene sorption in sediments, Environ. Sci. Technol., 39 (2005) 764–769.
[41] X.D. Zhu, Y.C. Liu, C. Zhou, G. Luo, S.C. Zhang, J.M. Chen, A novel porous carbon derived from hydrothermal carbon for efficient adsorption of tetracycline, Carbon, 77 (2014) 627–636.
[42] W.S. Carvalho, D.F. Martins, F.R. Gomes, I.R. Leite, L.G. Silva, R. Ruggiero, Phosphate adsorption on chemically modified sugarcane bagasse fibres, Biomass Bioenerg., 35 (2011) 3913–3919.
[43] P. Kulshrestha, R.F. Giese Jr., D.S. Aga, Investigating the molecular interactions of oxytetracycline in clay and organic matter: Insights on factors affecting its mobility in soil, Environ. Sci. Technol., 38 (2004) 4097–4105.
[44] H.J. Liu, Y. Yang, J. Kanf, M.H. Fan, J.H. Qu, Removal of tetracycline from water by Fe-Mn binary oxide, J. Environ. Sci., 24(2) (2012) 242–247.
[45] M. Teixidó, J.J. Pignatello, J.L. Beltrán, M. Granados, J. Peccia, Speciation of the ionizable antibiotic sulfamethazine on black carbon (biochar), Environ. Sci. Technol., 45 (2011) 10020–10027.
[46] H. Zheng, Z.Y. Wang, J. Zhao, H. Stephen, B.S. Xing, Sorption of antibiotic sulfamethoxazole varies with biochars produced at different temperatures, Environ. Pollut., 181 (2013) 60–67.
[47] X.R. Jing, Y.Y. Wang, W.J. Liu, Y.K. Wang, H. Jiang, Enhanced adsorption performance of tetracycline in aqueous solutions by methanol-modified biochar, Chem. Eng. J., 248 (2014) 168–174.
[48] S. Lagergren, Zurtheorie der sogenannten adsorption gelösterstoffe. Kungliga Svenska Vetenskapsakademiens, Handlinga, 24 (1898) 1–39.
[49] Y.S. Ho, G. McKay, Pseudo-second-order model for sorption process, Process Biochem., 34 (1999) 451–465.
[50] I. Langmuir, Kinetic model for the sorption of dye aqueous solution by clay-wood sawdust mixture, J. Am. Chem. Soc., 38 (1916) 2221–2295.
[51] H.M.F. Freundlich, Uber die adsorption in lasungen, J. Phys. Chem., 57 (1906) 385–470.